

COMMUNICATION

[View Article Online](#)
[View Journal](#) | [View Issue](#)

Cite this: *Nanoscale Adv.*, 2024, **6**, 1065

Received 13th December 2023
Accepted 18th January 2024

DOI: 10.1039/d3na01112g
rsc.li/nanoscale-advances

Polyacrylonitrile as a versatile matrix for gold nanoparticle-based SERS substrates

Saloni Sharma,^a Rajesh Kumar ^{*b} and Ram Manohar Yadav ^{*ac}

As an effective and ultrasensitive molecule detection technique, surface-enhanced Raman spectroscopy (SERS) needs efficient and highly responsive substrates to further enhance its sensitivity and utility. In this work, the preparation and characterisation of polyacrylonitrile/gold nanoparticle (PAN/AuNPs) composite porous films have been described for SERS-based detection of methylene blue (MB) dye. The PAN/AuNPs composite films were prepared with a simple dip coating technique, yielding a highly porous structure with uniformly dispersed Au nanoparticles (AuNPs). Scanning electron microscopy (SEM) revealed a linked pore network within the films. In X-ray diffraction (XRD), the characteristic crystal peak of AuNP clusters was observed, proving the presence of AuNPs in the composite. UV-vis absorption spectra also indicated the existence of the AuNPs. The methylene blue (MB) dye has been detected using PAN/AuNPs composite SERS substrates. These substrates showed excellent sensitivity by detecting 50 nM dye concentration and enhancing the Raman peak intensity at 1622 cm^{-1} . The SERS enhancement factor (EF) for MB detection was determined to be around 10^6 , demonstrating the remarkable sensitivity of the PAN/AuNPs composite porous films. The findings demonstrate the enormous potential of PAN/AuNPs composite porous films as reliable SERS substrates, displaying their efficacy in detecting trace levels of analytes in chemical and biological sensing applications.

1. Introduction

The research field of molecular sensing has been fundamentally transformed by surface-enhanced Raman spectroscopy (SERS), which uses ultrasensitive detection and identification of analytes at the single-molecule level.¹⁻⁴ The method is primarily based on the localised surface plasmon resonance (LSPR) phenomenon.^{5,6}

LSPR occurs when molecules are in close proximity to nanostructures made of noble metals, which causes the Raman signal to be amplified.^{7,8} SERS uses the electromagnetic and chemical phenomena that occur when analyte molecules are near nanostructures to amplify Raman signals.⁹⁻¹⁶

Gold nanoparticles (AuNPs) have been widely employed in SERS substrates because of their exceptional plasmonic properties, high chemical stability, and ease of functionalization.¹⁷⁻²³ LSPR is one of their unique optical properties that can considerably amplify the Raman signals of surrounding analyte molecules. By carefully controlling their size, shape, and interparticle spacing, AuNPs may be made to exhibit LSPR, making them ideal candidates for boosting SERS signals. Au has been widely employed in SERS active substrates by numerous researchers.²⁴⁻³¹ However, synthesizing AuNPs has always been challenging due to the tedious routes and use of harsh chemicals.³²⁻³⁸ Here, gold nanoparticles (AuNPs) are synthesised from gold chloride hydrate ($\text{HAuCl}_4 \cdot 3\text{H}_2\text{O}$) using a simple and straightforward approach utilizing dimethylformamide (DMF).³⁹⁻⁴¹ Using DMF as a solvent and reducing agent, it has been previously shown that the metallic nanostructures of gold, silver, and other metals can form in various ways.⁴²⁻⁴⁴ Here, a simple pathway has been introduced to synthesize AuNPs directly in PAN/DMF solution. This approach has the benefit of being a surfactant-free synthesis. Meanwhile, polymer nanocomposites not only enhance the overall surface properties but also give support to the reusable film.⁴⁵

Polyacrylonitrile (PAN) has good mechanical qualities, chemical stability, and processability, which make it suitable for SERS applications as a base material.⁴⁶⁻⁵² Using PAN as the composite matrix allows for the immobilisation of metal particles while preserving and even enhancing their strength and SERS performance. In addition, PAN films have a tendency to be porous due to their structure during deposition. The pores in films can facilitate the deposition of photonic materials at precisely regulated locations.⁵³⁻⁵⁶ The SERS-active sites may be improved through controlled deposition, which results in uniformly sized and packed AuNPs. The interaction volume

^aDepartment of Physics, VSSD College, CSJM University, Kanpur 208002, U.P., India

^bDepartment of Mechanical Engineering, Indian Institute of Technology, Kanpur 208016, U.P., India. E-mail: rajeshbhu1@gmail.com

^cDepartment of Physics, University of Allahabad, Prayagraj 211002, U.P., India. E-mail: rmyadav@alluniv.ac.in



between the analyte and the SERS-active substrate can be increased owing to the porous PAN layer, which can facilitate the penetration of analyte molecules into the pores. The sensitivity of SERS measurements improves, and so does the signal-to-noise ratio.

Methylene blue (MB) dye has been tested as an analyte which is utilized in many industrial domains due to its vivid blue colour, especially in paper and textiles.^{57–59} When appropriately handled for medical and research purposes, MB is considered relatively non-toxic to people. However, its use in higher dosages may harm the environment and human health. Usually, the water contaminated by MB dye is discharged into aquatic bodies by industrial wastes. Monitoring the presence of MB is crucial for assessing its effects on the environment and for fixing effective mitigating measures. Also, to safeguard aquatic life, it is important to find MB in wastewater.^{60,61}

So far, a number of different strategies have been suggested for the detection of dyes, such as colorimetry, fluorescence spectroscopy, thin-layer chromatography (TLC), ultraviolet-visible spectroscopy, high-performance liquid chromatography (HPLC), and a number of electrochemical approaches.^{62–72} However, because of their intricate construction, these instruments alter water molecules' physical and chemical properties, giving false readings. Therefore, the necessity for a more approachable strategy has drawn researchers to SERS.^{73–79} Due to the distinctive fingerprints of each dye, SERS can offer excellent selectivity in complex dye mixtures.⁸⁰

Systematically analysing the results of this research will aid in the development of PAN/AuNPs composite materials for SERS applications that are highly efficient for the detection of MB. The formation of a PAN/AuNPs composite film for SERS applications is the primary goal of this study. It was intended to observe the fabrication process to study the composite morphology, including the distribution of AuNPs inside the PAN matrix. The composite film was characterized for its structural and optical characteristics through sophisticated spectroscopic and microscopy techniques. It was simultaneously tested as a SERS substrate and the composite's effectiveness in detecting and identifying MB analyte was assessed. This research will help to improve molecular sensing technologies based on SERS, enabling sensitive and targeted detection in biomedical diagnostics, environmental monitoring, and food safety.^{26,81–97}

2. Experimental section

2.1. Materials/chemicals

Dimethylformamide (DMF) solution and polyacrylonitrile (PAN) (molecular weight: 150 000) were acquired from SRL Chemicals and Sigma Aldrich, respectively. DMF has a density of 0.947–0.949 g ml^{−1} with 99% purity, and PAN has a density of 1.184 g ml^{−1} at 25 °C. Finar Chemicals provided methylene blue (molecular weight: 373.9) and gold chloride (HAuCl₄·3H₂O) (molecular weight = 393.83) for the experiment.

2.2. Preparation of the PAN/AuNPs composite and its film

Fig. 1 shows the schematic illustration for the formation of the PAN/AuNPs composite and its film using the dip coating technique. Initially, 10% PAN solution was made by combining 1 g of PAN powder with 10 ml of DMF solvent. The solution was continuously stirred at 50 °C for 2 h to ensure that PAN was entirely dissolved in the solvent and a transparent solution had been obtained. A 20 mM aqueous gold chloride (HAuCl₄·3H₂O) solution was carefully mixed with a polyacrylonitrile (PAN) solution to create a composite solution. While the PAN/DMF combination was being stirred at 50 °C, 1 ml of the 20 mM gold chloride solution was gradually added. This caused the gold chloride to be reduced, vividly changing the solution's colour to a distinctive red, which indicates the creation of gold nanoparticles (AuNPs). Surprisingly, the AuNPs spontaneously clustered without stabilising or capping agents. Making use of this special method, a thin composite film was painstakingly created. This straightforward process probably influences further research or applications in areas like materials science or nanotechnology, where regulated nanoparticle assembly is essential.

The thin film was coated with a dip coating process. The glass substrate was dipped into the produced composite solution for 30 seconds at a speed of 3 mm s^{−1}. Following this process, the composite solution was consistently applied to the substrate. The PAN/AuNPs composite films were then heated at 75 °C for two hours for annealing.

2.3. Characterization

The pure PAN and PAN/AuNPs composite film crystal structures were examined by X-ray diffraction (XRD: PANalytical, X'Pert3 Power) with Cu-K radiation, $\lambda = 1.54$ Å in the selected 2θ range ($2\theta = 10$ –50°) at a scanning rate of 0.01° s^{−1}. Field-emission scanning electron microscopy (FESEM) was used to analyze the surface morphology and microstructure of the PAN and its composite films (FESEM: Carl Zeiss MERLIN VP Compact). The accelerating voltage used to produce the FESEM images was 5 kV. The optical properties of the films were tested with Agilent Cary 5000 UV spectrometer equipment. It was used to conduct UV-visible absorption spectroscopy in the UV to NIR region (200–600 nm).

Various concentrations of MB solutions in methanol, from 5 nM to 5 mM, were produced for the SERS experiment. Two microliters of MB dilutions were dropped and dried on pure PAN and PAN/AuNPs composite-based films and were examined in the SERS experiment. A confocal microscope with a 100× objective lens housed in a WITec alpha 300 Raman instrument was used to record SERS signals at room temperature. An excitation laser (Nd-YAG laser, 532 nm, 40 mW) was used to excite the substrate plasmons to collect the enhanced SERS data, with a 1 second accumulation time for each measurement.

3. Results and discussion

3.1. Structural characterization

3.1.1. Characterization of the PAN/AuNPs composite film. As shown in Fig. 2, the surface morphology of PAN and PAN/



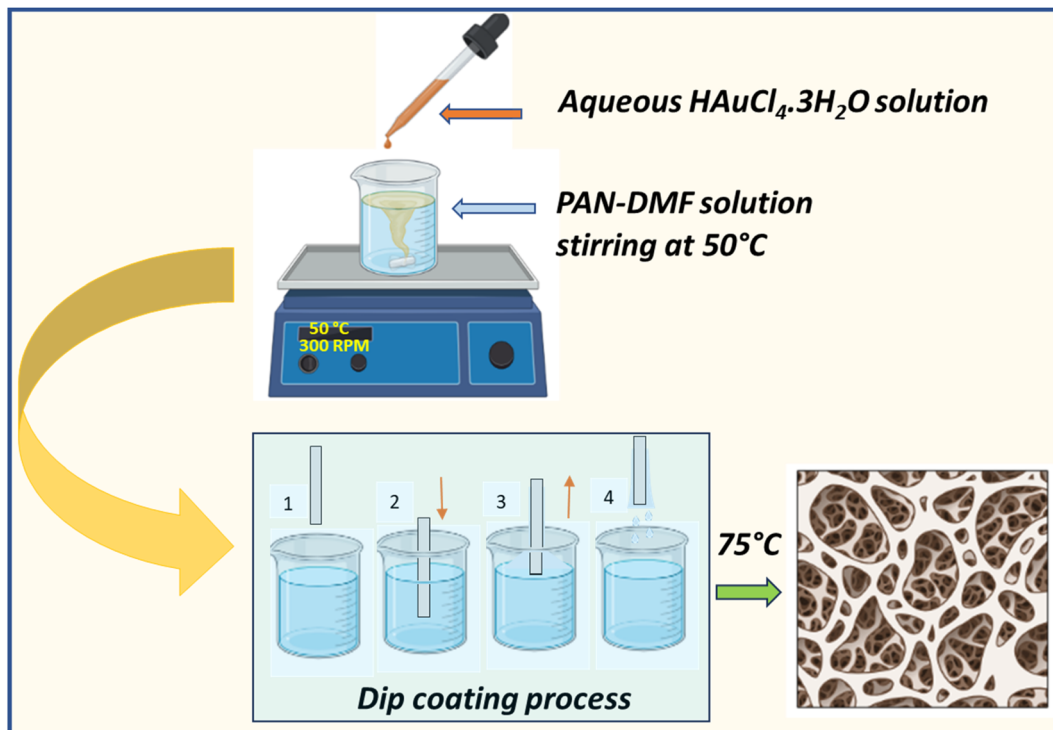


Fig. 1 Schematic representation of SERS substrate preparation.

AuNPs composites was examined using FESEM. FESEM images show that the films of PAN and PAN/AuNPs composites displayed complex porous patterns that contain micron-

sized length cavities. Despite there being striking visual similarities between PAN and PAN/AuNPs composite films, the PAN/AuNPs composite showed improved porosity and

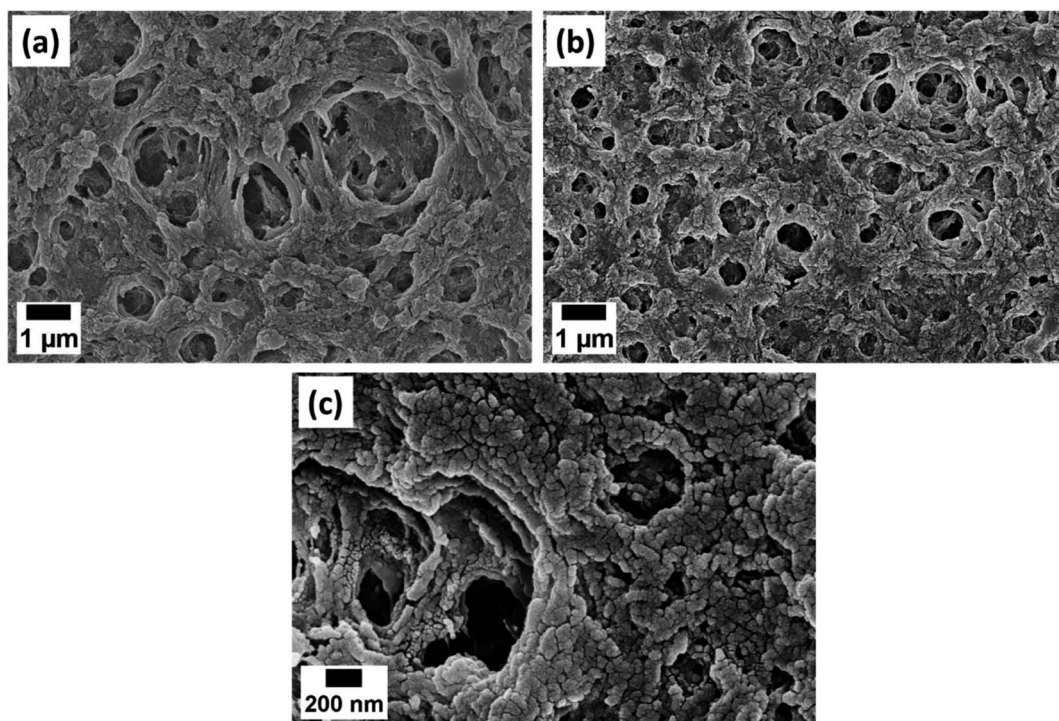


Fig. 2 FESEM images of (a) PAN, (b) PAN/AuNPs composite film at 25k \times magnification and (c) PAN/AuNPs composite film at 100k \times magnification.



luminosity around the pore edges. The enhancement in the number of pores may be credited to the addition of AuNPs, which allowed for clear differentiation. It is expected that all AuNPs were covered by the polymer matrix and thus did not appear on the surfaces of the PAN/AuNPs composite film as seen in the SEM micrographs (Fig. 2b and c).

Fig. 3a displays the X-ray diffraction (XRD) pattern of PAN and PAN/AuNPs composites. The (100) crystal plane of PAN is shown by a significant high-intensity diffraction peak in the XRD spectrum of PAN at $2\theta = 17.1^\circ$. However, the diffraction peak intensity reduces when AuNPs are added to PAN. The AuNP (111) crystal plane is also represented by a small diffraction peak at 38.1° . The cluster formation of the AuNPs, which subsequently lowers the overall crystallinity of the PAN/AuNPs composite, is responsible for the decrease of the diffraction peak intensity in the PAN/AuNPs composite. Due to the presence of AuNPs, this phenomenon was accompanied by converting some of the PAN crystalline areas into a less crystalline phase. As seen in Fig. 3b from the absorption spectra of UV-visible spectroscopy, AuNPs in cluster form were absorbed by the PAN polymer.

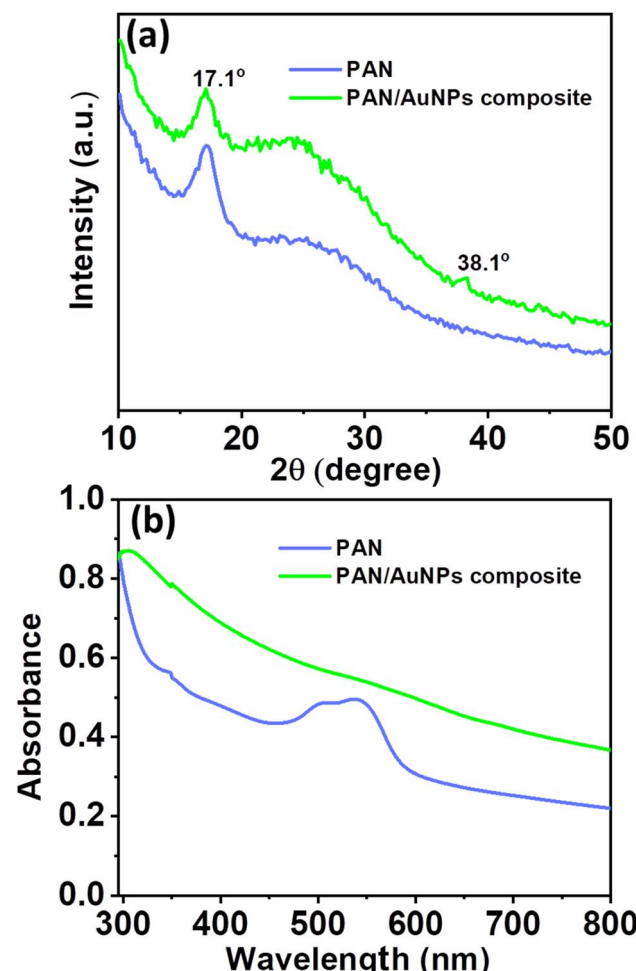


Fig. 3 (a) XRD and (b) UV visible spectra of PAN and PAN/AuNPs composite film.

3.2. Surface-enhanced Raman spectra (SERS) from methylene blue (MB)

A significantly enhanced signal of the MB peak at 1622 cm^{-1} was observed on SERS substrates produced by adding an aqueous 20 mM Au solution to the PAN/DMF solution and MB concentrations as low as 50 nM could be detected (Fig. 4a). The SERS amplification shown in the PAN/AuNPs composite porous films may be caused by the unique properties of the AuNPs embedded within the porous PAN matrix. The inclusion of AuNPs in the PAN matrix creates the LSPR effect, which is responsible for the enhancement. There may be several "hot spots" where electromagnetic enhancement greatly amplifies the Raman signals of MB molecules due to the porous structure of the film, which offers a sizable surface area. The uniform distribution of SERS-active sites produced by the dispersion of AuNPs throughout the PAN matrix ensures consistent and repeatable SERS signals. The strong interaction between MB molecules and the AuNPs further enhances the SERS effect, leading to the observed EF value of 10^6 (Fig. 4a).

Hence, the porous structure and the development of hot spots could be the two main causes of the amplification of MB molecule SERS signals in the PAN/AuNPs composite films as explained in Fig. 4b. The PAN/AuNPs composite films have a highly porous structure with multiple linked voids and pores

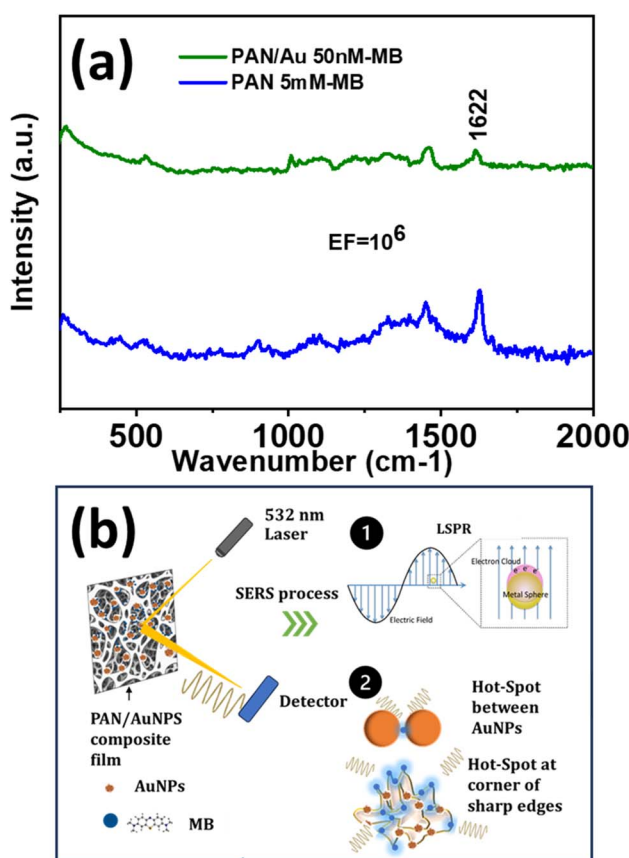


Fig. 4 (a) SERS spectra of pure PAN and PAN/AuNPs composite film tested with MB and (b) schematic representation of SERS related observations.



all over the substance. The large surface areas offered by the porous PAN/AuNPs composite result in a large number of spaces and edges where MB molecules can be adsorbed. The high surface area to volume ratio increases the likelihood of analyte–nanoparticle interactions and SERS activity. Because there are more scattering events, MB molecule's SERS signals are amplified, producing stronger Raman intensity. Furthermore, the porosity model makes it simple for MB molecules to permeate the film, increasing the analyte accessibility to the AuNPs incorporated into the PAN matrix.

In the presence of AuNPs in the PAN matrix, strong electromagnetic fields are formed around the NPs due to LSPR effects (Fig. 4b). These electromagnetic fields are stronger at “hot spots,” and these hot spots have a high concentration of electromagnetic energy, which amplifies the Raman signals of nearby molecules like MB. Due to the significant electromagnetic field augmentation, their Raman scattering signals are greatly enhanced when MB molecules are adsorbed onto these hot spots or sharp corners (Fig. 4a). The chemical interaction between the analyte and the AuNPs is improved by the LSPR-induced hot spots, which function as nanoscale antennas. The enhanced sensitivity and detection capabilities of the system are the result of enhanced energy transfer and Raman scattering made possible by the increased contact.

Therefore, the PAN/AuNPs composite porous films also have good repeatability and stability, making them acceptable for real-world molecular sensing and detection uses. Their capacity for large-scale production is further increased by the simple and affordable synthesis process.

The enhancement factor (EF) can be calculated by

$$EF = (I_{SERS}/I_{Raman})(N_b/N_{ads}) \quad (1)$$

where I_{SERS} is the signal intensity of SERS spectra, I_{Raman} the signal intensity of normal Raman spectra, N_b the number of molecules on the bulk sample and N_{ads} the number of probed molecules contributing to SERS.

4. Conclusions

In this investigation, Surface-Enhanced Raman Spectroscopy (SERS) was employed to assess the effectiveness of PAN/AuNPs composites in detecting methylene blue (MB). The utilization of SERS with AuNPs proved to be a highly effective analytical approach for the detection of methylene blue (MB) with remarkable sensitivity and specificity. The dip-coated PAN/AuNPs composite film displayed an enhanced SERS signal of MB at 1622 cm^{-1} , which was remarkably increased with an EF of 10^6 when 50 nM MB solution was tested. The strong electromagnetic fields produced by Localized Surface Plasmon Resonance (LSPR) surrounding the hotspot and porous structure may be responsible for the increased sensitivity. The composite porous films of PAN and AuNPs demonstrated remarkable stability and repeatability, making them appropriate for real-world uses in various pollutants and molecular sensing and detection. Their simple and economical synthesis procedure further enhances their potential for large-scale production.

Conflicts of interest

There are no conflicts to declare.

References

- 1 H. Pu, W. Xiao and D. W. Sun, SERS-microfluidic systems: A potential platform for rapid analysis of food contaminants, *Trends Food Sci. Technol.*, 2017, **70**, 114–126, DOI: [10.1016/J.TIFS.2017.10.001](https://doi.org/10.1016/J.TIFS.2017.10.001).
- 2 V. S. Vendamani, S. V. S. N. Rao, A. P. Pathak and V. R. Soma, Robust and cost-effective silver dendritic nanostructures for SERS-based trace detection of RDX and ammonium nitrate, *RSC Adv.*, 2020, **10**, 44747–44755, DOI: [10.1039/d0ra08834j](https://doi.org/10.1039/d0ra08834j).
- 3 R. Mishra, R. K. Pandey, S. Jana, C. Upadhyay and R. Prakash, Synthesis of uniformly dispersed large area polymer/AgNPs thin film at air–liquid interface for electronic application, *Mater. Today Commun.*, 2020, **24**, 101191, DOI: [10.1016/j.mtcomm.2020.101191](https://doi.org/10.1016/j.mtcomm.2020.101191).
- 4 G. Zhdanov, E. Nyhrikova, N. Meshcheryakova, O. Kristavchuk, A. Akhmetova, E. Andreev, E. Rudakova, A. Gambaryan, I. Yaminsky, A. Aralov, V. Kukushkin and E. Zavyalova, A Combination of Membrane Filtration and Raman-Active DNA Ligand Greatly Enhances Sensitivity of SERS-Based Aptasensors for Influenza A Virus, *Front. Chem.*, 2022, **10**, 937180, DOI: [10.3389/fchem.2022.937180](https://doi.org/10.3389/fchem.2022.937180).
- 5 F. Hu, T. Li, T. Sun, Y. Liu, D. Yu, R. Jia, L. Shi and L. Huang, Localized surface plasmon resonance effect driven fabrication of core/shell Au NRs@MnO₂ nanosheets, *Mater. Today Commun.*, 2021, **28**, 102535, DOI: [10.1016/j.mtcomm.2021.102535](https://doi.org/10.1016/j.mtcomm.2021.102535).
- 6 B. Zhu, X. Feng, L. Chen, W. Luo, B. Fang, C. Yuan, C. Zhou, J. Zhao and G. Rao, Simulation of LSPR optical and electric field enhancement distribution based on gold nanobipyramids using a modified nanosphere, *Mater. Today Commun.*, 2022, **32**, 104136, DOI: [10.1016/j.mtcomm.2022.104136](https://doi.org/10.1016/j.mtcomm.2022.104136).
- 7 N. Mhlanga and T. A. Ntho, A theoretical study of 4-Mercaptobenzoic acid assembled on Ag for surface-enhanced raman scattering applications, *Mater. Today Commun.*, 2021, **26**, 101698, DOI: [10.1016/j.mtcomm.2020.101698](https://doi.org/10.1016/j.mtcomm.2020.101698).
- 8 E. V. Solovyeva, O. V. Odintsova, V. O. Svinko, D. V. Makeeva and D. V. Danilov, Hydroxyapatite-nanosilver composites with plasmonic properties for application in surface-enhanced Raman spectroscopy, *Mater. Today Commun.*, 2023, **35**, 105908, DOI: [10.1016/j.mtcomm.2023.105908](https://doi.org/10.1016/j.mtcomm.2023.105908).
- 9 N. Mudgal, A. Saharia, A. Agarwal and G. Singh, ZnO and Bimetallic (Ag–Au) Layers Based Surface Plasmon Resonance (SPR) Biosensor with BaTiO₃ and Graphene for Biosensing Applications, *IETE J. Res.*, 2020, **69**(2), 932–939, DOI: [10.1080/03772063.2020.1844074](https://doi.org/10.1080/03772063.2020.1844074).
- 10 G. C. Schatz, M. A. Young and R. P. Van Duyne, Electromagnetic Mechanism of SERS, *Surface-Enhanced Raman Scattering*, 2006, pp. 19–45, DOI: [10.1007/3-540-33567-6_2](https://doi.org/10.1007/3-540-33567-6_2).



11 L. Fabris, Gold-based SERS tags for biomedical imaging, *J. Opt.*, 2015, **17**, 114002, DOI: [10.1088/2040-8978/17/11/114002](https://doi.org/10.1088/2040-8978/17/11/114002).

12 E. C. Le Ru and P. G. Etchegoin, Sub-wavelength localization of hot-spots in SERS, *Chem. Phys. Lett.*, 2004, **396**, 393–397, DOI: [10.1016/j.cplett.2004.08.065](https://doi.org/10.1016/j.cplett.2004.08.065).

13 D. Franco, L. M. De Plano, M. G. Rizzo, S. Scibilia, G. Lentini, E. Fazio, F. Neri, S. P. P. Guglielmino and A. M. Mezzasalma, Bio-hybrid gold nanoparticles as SERS probe for rapid bacteria cell identification, *Spectrochim. Acta, Part A*, 2020, **224**, 117394, DOI: [10.1016/j.saa.2019.117394](https://doi.org/10.1016/j.saa.2019.117394).

14 V. Van Cat, N. X. Dinh, L. T. Tam, N. Van Quy, V. N. Phan and A.-T. Le, One-pot hydrothermal-synthesized rGO-Ag nanocomposite as a sensing platform for detection and quantification of methylene blue organic dye and tricyclazole pesticide, *Mater. Today Commun.*, 2019, **21**, 100639, DOI: [10.1016/j.mtcomm.2019.100639](https://doi.org/10.1016/j.mtcomm.2019.100639).

15 R. Prabhu B, C. Kavitha and N. S. John, Ag decorated sea urchin-MoO₃ based hierarchical micro-nano structures as surface – enhanced Raman spectroscopy substrates for the detection of a nitrosamine industrial pollutant, *Mater. Today Commun.*, 2022, **33**, 104995, DOI: [10.1016/j.mtcomm.2022.104995](https://doi.org/10.1016/j.mtcomm.2022.104995).

16 X. Cheng, J. Jin, M. Shi, M. Ge, J. Miao, C. Ci, Z. Xue and P. Dong, Facile synthesis of large-scale TiO₂ nanorod arrays decorated with Ag nanoparticles as sensitive 3D SERS substrates, *Mater. Today Commun.*, 2023, **35**, 106088, DOI: [10.1016/j.mtcomm.2023.106088](https://doi.org/10.1016/j.mtcomm.2023.106088).

17 A. Jakhmola, S. Krishnan, V. Onesto, F. Gentile, M. Profeta, A. Manikas, E. Battista, R. Vecchione and P. A. Netti, Sustainable synthesis and theoretical studies of polyhedral gold nanoparticles displaying high SERS activity, NIR absorption, and cellular uptake, *Mater. Today Chem.*, 2022, **26**, 101016, DOI: [10.1016/j.mtchem.2022.101016](https://doi.org/10.1016/j.mtchem.2022.101016).

18 S. Siddiqui, J. H. Niazi and A. Qureshi, Mn₃O₄-Au nanozymes as peroxidase mimic and the surface-enhanced Raman scattering nanosensor for the detection of hydrogen peroxide, *Mater. Today Chem.*, 2021, **22**, 100560, DOI: [10.1016/j.mtchem.2021.100560](https://doi.org/10.1016/j.mtchem.2021.100560).

19 A. Jakhmola, R. Vecchione, F. Gentile, M. Profeta, A. C. Manikas, E. Battista, M. Celentano, V. Onesto and P. A. Netti, Experimental and theoretical study of biodirected green synthesis of gold nanoflowers, *Mater. Today Chem.*, 2019, **14**, 100203, DOI: [10.1016/j.mtchem.2019.100203](https://doi.org/10.1016/j.mtchem.2019.100203).

20 T. Wang, H.-M. Li, B.-Y. Wen, R. Panneerselvam, Y.-J. Zhang, A. Wang, F.-L. Zhang, S. Jin and J.-F. Li, Au nanocakes as a SERS sensor for on site and ultrafast detection of dioxins, *Vib. Spectrosc.*, 2023, **126**, 103518, DOI: [10.1016/j.vibspec.2023.103518](https://doi.org/10.1016/j.vibspec.2023.103518).

21 S. Wang, H. Jiang, J. Feng, Y. Jin, F. An, L. Zhu and A. Xiao, Hierarchical metal-dielectric-metal nanostructures as SERS sensors for sensitive detection of polycyclic aromatic hydrocarbons, *Appl. Surf. Sci.*, 2024, **646**, 158926, DOI: [10.1016/j.apsusc.2023.158926](https://doi.org/10.1016/j.apsusc.2023.158926).

22 R. M. C. R. Ramos, W. Jiang, J. Z. X. Heng, H. Y. Y. Ko, E. Ye and M. D. Regulacio, Hyperbranched Au Nanocorals for SERS Detection of Dye Pollutants, *ACS Appl. Nano Mater.*, 2023, **6**, 3963–3973, DOI: [10.1021/acsanm.3c00192](https://doi.org/10.1021/acsanm.3c00192).

23 H. N. Tran, N. B. Nguyen, N. H. Ly, S.-W. Joo and Y. Vasseghian, Core-shell Au@ZIF-67-based pollutant monitoring of thiram and carbendazim pesticides, *Environ. Pollut.*, 2023, **317**, 120775, DOI: [10.1016/j.envpol.2022.120775](https://doi.org/10.1016/j.envpol.2022.120775).

24 G. P. Szekeres and J. Kneipp, SERS probing of proteins in gold nanoparticle agglomerates, *Front. Chem.*, 2019, **7**, 30, DOI: [10.3389/fchem.2019.00030](https://doi.org/10.3389/fchem.2019.00030).

25 D. Majumdar, S. Jana and S. Kumar Ray, Gold nanoparticles decorated 2D-WSe₂ as a SERS substrate, *Spectrochim. Acta, Part A*, 2022, **278**, 121349, DOI: [10.1016/j.saa.2022.121349](https://doi.org/10.1016/j.saa.2022.121349).

26 N. Ha Anh, M. Quan Doan, N. Xuan Dinh, T. Quang Huy, D. Quang Tri and A. T. Le, Gold nanoparticles-based SERS nanosensor for thiram and chloramphenicol monitoring in food samples: Insight into effects of analyte molecular structure on their sensing performance and signal enhancement, *Appl. Surf. Sci.*, 2022, **584**, 152555, DOI: [10.1016/j.apsusc.2022.152555](https://doi.org/10.1016/j.apsusc.2022.152555).

27 G. Yang, X. Fang, Q. Jia, H. Gu, Y. Li, C. Han and L. L. Qu, Fabrication of paper-based SERS substrates by spraying silver and gold nanoparticles for SERS determination of malachite green, methylene blue, and crystal violet in fish, *Microchim. Acta*, 2020, **187**, 310, DOI: [10.1007/s00604-020-04262-2](https://doi.org/10.1007/s00604-020-04262-2).

28 Q. Ke, L. Chen, B. Fang, Y. Chen and W. Zhang, Simulating electric field intensity distribution of LSPR based on gold nanobipyramids, *Mater. Today Commun.*, 2021, **26**, 101953, DOI: [10.1016/j.mtcomm.2020.101953](https://doi.org/10.1016/j.mtcomm.2020.101953).

29 A. Atapour, H. Khajehzadeh, M. Shafie, M. Abbasi, S. Mosleh-Shirazi, S. R. Kasaee and A. M. Amani, Gold nanoparticle-based aptasensors: A promising perspective for early-stage detection of cancer biomarkers, *Mater. Today Commun.*, 2022, **30**, 103181, DOI: [10.1016/j.mtcomm.2022.103181](https://doi.org/10.1016/j.mtcomm.2022.103181).

30 M. Deb, R. Hunter, M. Taha, H. Abdelbary and H. Anis, Rapid detection of bacteria using gold nanoparticles in SERS with three different capping agents: Thioglucose, polyvinylpyrrolidone, and citrate, *Spectrochim. Acta, Part A*, 2022, **280**, 121533, DOI: [10.1016/j.saa.2022.121533](https://doi.org/10.1016/j.saa.2022.121533).

31 F. M. M. Aldosari, Characterization of Labeled Gold Nanoparticles for Surface-Enhanced Raman Scattering, *Molecules*, 2022, **27**, 892, DOI: [10.3390/molecules27030892](https://doi.org/10.3390/molecules27030892).

32 A. Galdamez, A. Serrano, G. Santana, N. Arjona, L. G. Arriaga, J. Tapia Ramirez, G. Oza and A. Dutt, DNA probe functionalization on different morphologies of ZnO/Au nanowire for bio-sensing applications, *Mater. Lett.*, 2019, **235**, 250–253, DOI: [10.1016/J.MATLET.2018.10.026](https://doi.org/10.1016/J.MATLET.2018.10.026).

33 M. Akbarian, M. Gholinejad, S. Mohammadi-Samani and F. Farjadian, Theranostic mesoporous silica nanoparticles made of multi-nuclear gold or carbon quantum dots particles serving as pH responsive drug delivery system, *Microporous Mesoporous Mater.*, 2022, **329**, 111512, DOI: [10.1016/J.MICROMESO.2021.111512](https://doi.org/10.1016/J.MICROMESO.2021.111512).

34 T. Mahaddalkar, S. Mehta, S. Cheriyamundath, H. Muthurajan and M. Lopus, Tryptone-stabilized gold nanoparticles target tubulin and inhibit cell viability by



inducing an unusual form of cell cycle arrest, *Exp. Cell Res.*, 2017, **360**, 163–170, DOI: [10.1016/j.yexer.2017.09.002](https://doi.org/10.1016/j.yexer.2017.09.002).

35 Y. Liang, C. Lin, A. Shen, R. Guo and Y. Li, Porous POM/PLLA membranes decorated with gold nanoparticles as flexible and efficient plasmonic substrates for surface-enhanced Raman scattering, *Appl. Surf. Sci.*, 2019, **498**, 143856, DOI: [10.1016/jAPSUSC.2019.143856](https://doi.org/10.1016/jAPSUSC.2019.143856).

36 L. N. Nguyen, P. Lamichhane, E. H. Choi and G. J. Lee, Structural and Optical Sensing Properties of Nonthermal Atmospheric Plasma-Synthesized Polyethylene Glycol-Functionalized Gold Nanoparticles, *Nanomaterials*, 2021, **11**, 1678, DOI: [10.3390/NANO11071678](https://doi.org/10.3390/NANO11071678).

37 P. Wang, L. Zhang, Y. Xia, L. Tong, X. Xu and Y. Ying, Polymer Nanofibers Embedded with Aligned Gold Nanorods: A New Platform for Plasmonic Studies and Optical Sensing, *Nano Lett.*, 2012, **12**, 3145–3150, DOI: [10.1021/NL301055F](https://doi.org/10.1021/NL301055F).

38 Y. Xiao, C. Wang, K. Liu, L. Wei, Z. Luo, M. Zeng and Y. Yi, Promising pure gold aerogel: *in situ* preparation by composite sol-gel and application in catalytic removal of pollutants and SERS, *J. Solgel. Sci. Technol.*, 2021, **99**, 614–626, DOI: [10.1007/s10971-021-05597-9](https://doi.org/10.1007/s10971-021-05597-9).

39 H. Rajput, A. Kedia, D. Shah and N. Sharma, Exploiting Reducing Ability of DMF For Assembled Gold Nanostructures, *Mater. Res. Proc.*, 2022, **22**, 102–108, DOI: [10.21741/9781644901878-14](https://doi.org/10.21741/9781644901878-14).

40 M. Schulz-Dobrick, K. V. Sarathy and M. Jansen, Surfactant-free synthesis and functionalization of gold nanoparticles, *J. Am. Chem. Soc.*, 2005, **127**, 12816–12817, DOI: [10.1021/ja054734t](https://doi.org/10.1021/ja054734t).

41 S. P. Cho, S. Jang, H. N. Jo, S. A. Lee, S. Bae, S. H. Lee, J. Hwang, H. I. Joh, G. Wang and T. W. Kim, One step synthesis of Au nanoparticle-cyclized polyacrylonitrile composite films and their use in organic nano-floating gate memory applications, *J. Mater. Chem. C*, 2016, **4**, 1511–1516, DOI: [10.1039/C5TC04166J](https://doi.org/10.1039/C5TC04166J).

42 I. Pastorizo-Santos and L. M. Liz-Marzán, *N,N*-Dimethylformamide as a Reaction Medium for Metal Nanoparticle Synthesis, *Adv. Funct. Mater.*, 2009, **19**, 679–688, DOI: [10.1002/ADFM.200801566](https://doi.org/10.1002/ADFM.200801566).

43 J. Liu, W. Ong, A. E. Kaifer and C. Peinador, A “macrocyclic effect” on the formation of capped silver nanoparticles in DMF, *Langmuir*, 2002, **18**, 5981–5983, DOI: [10.1021/la025956x](https://doi.org/10.1021/la025956x).

44 I. Pastoriza-Santos and L. M. Liz-Marzán, Formation of PVP-Protected Metal Nanoparticles in DMF, *Langmuir*, 2002, **18**, 2888–2894, DOI: [10.1021/la015578g](https://doi.org/10.1021/la015578g).

45 R. M. Yadav, R. Kumar, K. Awasthi and O. N. Srivastava, Preparation of Carbon–Nitrogen Nanotubes (CNNTs)–Poly Ethylene Oxide (PEO) Composites Films and their Electrical Conductivity Measurement, *Int. J. Nanosci.*, 2011, **10**, 1091–1094, DOI: [10.1142/S0219581X11009477](https://doi.org/10.1142/S0219581X11009477).

46 E. Zussman, X. Chen, W. Ding, L. Calabri, D. A. Dikin, J. P. Quintana and R. S. Ruoff, Mechanical and structural characterization of electrospun PAN-derived carbon nanofibers, *Carbon*, 2005, **43**, 2175–2185, DOI: [10.1016/j.CARBON.2005.03.031](https://doi.org/10.1016/j.CARBON.2005.03.031).

47 H. Bisheh and Y. Abdin, Carbon Fibers: From PAN to Asphaltene Precursors; A State-of-Art Review, *C*, 2023, **9**, 19, DOI: [10.3390/C9010019](https://doi.org/10.3390/C9010019).

48 S. Saadati, U. Eduok, H. Westphalen, A. Abdelrasoul, A. Shoker, P. Choi, H. Doan, F. Ein-Mozaffari and N. Zhu, Assessment of polyethersulfone and polyacrylonitrile hemodialysis clinical membranes: *in situ* synchrotron-based imaging of human serum proteins adsorption, interaction analyses, molecular docking and clinical inflammatory biomarkers investigations, *Mater. Today Commun.*, 2021, **29**, 102928, DOI: [10.1016/j.mtcomm.2021.102928](https://doi.org/10.1016/j.mtcomm.2021.102928).

49 S. Sharma, R. Kumar and R. M. Yadav, Polyacrylonitrile/N-doped graphene quantum dots nanocomposite activity as SERS nanosensors for detection of methylene blue, *Mater. Today Commun.*, 2023, **36**, 106860, DOI: [10.1016/j.mtcomm.2023.106860](https://doi.org/10.1016/j.mtcomm.2023.106860).

50 M. Hajikhani, S. Kousheh, Y. Zhang and M. Lin, Design of a novel SERS substrate by electrospinning for the detection of thiabendazole in soy-based foods, *Food Chem.*, 2024, **436**, 137703, DOI: [10.1016/j.foodchem.2023.137703](https://doi.org/10.1016/j.foodchem.2023.137703).

51 S. M. Kong, D. Shin, J.-W. Oh, H. Park, J. S. Lee, N.-I. Won and Y. H. Na, One-pot platform for the collection and detection of nanoparticles: Flexible surface-enhanced Raman scattering (SERS) substrates with nano-pore structure, *Chem. Eng. J.*, 2023, **471**, 144753, DOI: [10.1016/j.cej.2023.144753](https://doi.org/10.1016/j.cej.2023.144753).

52 Y. Zhang, S. Zhou, J. Li, J. Chen, J. Chen and X. Huang, Ag/ZIF-8/polyacrylonitrile flexible SERS substrate with high sensitivity for the surface corrosion analysis, *Polym. Adv. Technol.*, 2024, **35**, e6255, DOI: [10.1002/pat.6255](https://doi.org/10.1002/pat.6255).

53 A. Virga, P. Rivolo, F. Frascella, A. Angelini, E. Descrovi, F. Geobaldo and F. Giorgis, Silver Nanoparticles on Porous Silicon: Approaching Single Molecule Detection in Resonant SERS Regime, *J. Phys. Chem. C*, 2013, **117**, 20139–20145, DOI: [10.1021/JP405117P](https://doi.org/10.1021/JP405117P).

54 C. El Bekkali, J. Labrag, A. Oulguidoum, I. Chamkhi, A. Laghzizil, J. M. Nunzi, D. Robert and J. Aurag, Porous ZnO/hydroxyapatite nanomaterials with effective photocatalytic and antibacterial activities for the degradation of antibiotics, *Nanotechnol. Environ. Eng.*, 2022, **7**, 333–341, DOI: [10.1007/s41204-021-00172-7](https://doi.org/10.1007/s41204-021-00172-7).

55 A. B. Radwan, S. I. El-Hout, M. A. M. Ibrahim, E. H. Ismail and A. M. Abdullah, Superior Corrosion and UV-Resistant Highly Porous Poly(vinylidene fluoride-co-hexafluoropropylene)/alumina Superhydrophobic Coating, *ACS Appl. Polym. Mater.*, 2022, **4**, 1358–1367, DOI: [10.1021/ACSAPM.1C01710](https://doi.org/10.1021/ACSAPM.1C01710).

56 H. Ko, S. Chang and V. V. Tsukruk, Porous Substrates for Label-Free Molecular Level Detection of Nonresonant Organic Molecules, *ACS Nano*, 2009, **3**, 181–188, DOI: [10.1021/nn800569f](https://doi.org/10.1021/nn800569f).

57 E. Bistas and D. K. Sanghavi, Methylene Blue, *History of Modern Clinical Toxicology*, 2023, pp. 231–241, DOI: [10.1016/B978-0-12-822218-8.00052-1](https://doi.org/10.1016/B978-0-12-822218-8.00052-1).

58 Y. N. Liu, X. Zhou, X. Wang, K. Liang, Z. K. Yang, C. C. Shen, M. Imran, S. Sahar and A. W. Xu, Hydrogenation/oxidation



induced efficient reversible color switching between methylene blue and leuco-methylene blue, *RSC Adv.*, 2017, **7**, 30080–30085, DOI: [10.1039/c7ra04498d](https://doi.org/10.1039/c7ra04498d).

59 R. Mohamat, S. Abu Bakar, A. Mohamed, Muqoyyanah, S. N. E. A. Mohamad Kamal, M. H. D. Othman, R. Rohani, M. H. Mamat, M. F. Malek, M. K. Ahmad and S. Ramakrishna, Methylene blue rejection and antifouling properties of different carbonaceous additives-based polyvinylidene fluoride membrane, *Mater. Today Commun.*, 2023, **35**, 105862, DOI: [10.1016/j.mtcomm.2023.105862](https://doi.org/10.1016/j.mtcomm.2023.105862).

60 A. Krishna Moorthy, B. Govindarajan Rathi, S. P. Shukla, K. Kumar and V. Shree Bharti, Acute toxicity of textile dye Methylene blue on growth and metabolism of selected freshwater microalgae, *Environ. Toxicol. Pharmacol.*, 2021, **82**, 103552, DOI: [10.1016/j.etap.2020.103552](https://doi.org/10.1016/j.etap.2020.103552).

61 M. Sakir, E. T. Akgul and M. Demir, Highly sensitive detection of cationic pollutants on molybdenum carbide (MXene)/Fe₂O₃/Ag as a SERS substrate, *Mater. Today Chem.*, 2023, **33**, 101702, DOI: [10.1016/j.mtchem.2023.101702](https://doi.org/10.1016/j.mtchem.2023.101702).

62 J. Müller-Maatsch, R. M. Schweiggert and R. Carle, Adulteration of anthocyanin- and betalain-based coloring foodstuffs with the textile dye 'Reactive Red 195' and its detection by spectrophotometric, chromatic and HPLC-PDA-MS/MS analyses, *Food Control*, 2016, **70**, 333–338, DOI: [10.1016/j.foodcont.2016.06.012](https://doi.org/10.1016/j.foodcont.2016.06.012).

63 T. Yurdun, R. Karadag, E. Dolen and M. S. Mubarak, Identification of natural yellow, blue, green and black dyes in 15th-17th centuries Ottoman silk and wool textiles by HPLC with diode array detection, *Rev. Anal. Chem.*, 2011, **30**, 153–164, DOI: [10.1515/revac.2011.101](https://doi.org/10.1515/revac.2011.101).

64 L. Exbrayat, B. Rameau, M. Uebel, M. Rohwerder, K. Landfester, D. Crespy, E. Campazzi, S. Touzain and J. Creus, New approach using fluorescent nanosensors for filiform corrosion inhibition, *Mater. Lett.*, 2022, **318**, 132240, DOI: [10.1016/j.matlet.2022.132240](https://doi.org/10.1016/j.matlet.2022.132240).

65 S. Selberg, E. Vanker, P. Peets, K. Wright, S. Tshepelevitsh, T. Pagano, S. Vahur, K. Herodes and I. Leito, Non-invasive analysis of natural textile dyes using fluorescence excitation-emission matrices, *Talanta*, 2023, **252**, 123805, DOI: [10.1016/j.talanta.2022.123805](https://doi.org/10.1016/j.talanta.2022.123805).

66 J. M. Park, S. J. Kim, J. H. Jang, Z. Wang, P. G. Kim, D. J. Yoon, J. Kim, G. Hansen and K. L. DeVries, Actuation of electrochemical, electro-magnetic, and electro-active actuators for carbon nanofiber and Ni nanowire reinforced polymer composites, *Composites, Part B*, 2008, **39**, 1161–1169, DOI: [10.1016/j.compositesb.2008.03.009](https://doi.org/10.1016/j.compositesb.2008.03.009).

67 S. C. M. Signorelli, J. M. Costa and A. F. de Almeida Neto, Electrocoagulation-flotation for orange II dye removal: Kinetics, costs, and process variables effects, *J. Environ. Chem. Eng.*, 2021, **9**, 106157, DOI: [10.1016/j.jece.2021.106157](https://doi.org/10.1016/j.jece.2021.106157).

68 V. Baiju, P. Abhishek, K. L. Priya and S. P. A. Mohammed, Performance investigation of silica gel based consolidated composite adsorbents effective for adsorption desalination systems, *Mater. Today Commun.*, 2022, **32**, 104015, DOI: [10.1016/j.mtcomm.2022.104015](https://doi.org/10.1016/j.mtcomm.2022.104015).

69 H. Montaseri and P. B. C. Forbes, Molecularly imprinted polymer coated quantum dots for fluorescence sensing of acetaminophen, *Mater. Today Commun.*, 2018, **17**, 480–492, DOI: [10.1016/j.mtcomm.2018.10.007](https://doi.org/10.1016/j.mtcomm.2018.10.007).

70 S. Sharma, R. Kumar and R. M. Yadav, Poly(vinylidene fluoride-hexafluoropropylene)/mesoporous graphitic carbon nitride composite membranes for photocatalytic methylene blue degradation and sensing applications, *Polym. Eng. Sci.*, 2023, **1**–11, DOI: [10.1002/pen.26571](https://doi.org/10.1002/pen.26571).

71 S. Sharma, S. S. Mishra, R. Kumar and R. M. Yadav, Recent progress on polyvinylidene difluoride-based nanocomposites: applications in energy harvesting and sensing, *New J. Chem.*, 2022, **46**, 18613–18646, DOI: [10.1039/D2NJ00002D](https://doi.org/10.1039/D2NJ00002D).

72 M. S. Yadav, Fabrication and characterization of supercapacitor electrodes using chemically synthesized CuO nanostructure and activated charcoal (AC) based nanocomposite, *J. Nanopart. Res.*, 2020, **22**, 303, DOI: [10.1007/s11051-020-05027-x](https://doi.org/10.1007/s11051-020-05027-x).

73 L. Chen, W. Luo, B. Fang, J. Sun, Y. Chen, X. Feng and W. Zhang, Searching for high similarity of longitudinal local surface plasmon resonance in gold and silver nanobipyramids, *Mater. Today Commun.*, 2022, **30**, 103173, DOI: [10.1016/j.mtcomm.2022.103173](https://doi.org/10.1016/j.mtcomm.2022.103173).

74 R. Feng, J. Meng, H. Yuan, X. Zhang, C. Gao, C. Ban, Y. Guo and K. Wang, Bi₅O₇Br-nanotube@Au-nanoparticle core-shell assembly for high signal-to-noise ratio SERS detection of adenine, *Mater. Today Commun.*, 2023, **34**, 105471, DOI: [10.1016/j.mtcomm.2023.105471](https://doi.org/10.1016/j.mtcomm.2023.105471).

75 A. Hariharan and P. Vadlamudi, SERS of norepinephrine: A computational and experimental study, *Mater. Today Commun.*, 2021, **27**, 102429, DOI: [10.1016/j.mtcomm.2021.102429](https://doi.org/10.1016/j.mtcomm.2021.102429).

76 L. Zhang, R. Zhao, Y. Wu, Z. Zhang, Y. Chen, M. Liu, N. Zhou, Y. Wang, X. Fu, X. Zhuang, J. Wang and L. Chen, Ultralow-background SERS substrates for reliable identification of organic pollutants and degradation intermediates, *J. Hazard. Mater.*, 2023, **460**, 132508, DOI: [10.1016/j.jhazmat.2023.132508](https://doi.org/10.1016/j.jhazmat.2023.132508).

77 B. Albini, M. Parmigiani, G. Pellegrini, A. Taglietti and P. Galinetto, Glass supported SERS chips for emerging pollutant analyses, *J. Mater. Sci.: Mater. Electron.*, 2023, **34**, 1619, DOI: [10.1007/s10854-023-11041-1](https://doi.org/10.1007/s10854-023-11041-1).

78 J. Ferreira de Sousa Junior, S. Columbus, J. Hammouche, K. Ramachandran, K. Daoudi and M. Gaidi, Engineered micro-pyramids functionalized with silver nanoarrays as excellent cost-effective SERS chemosensors for multi-hazardous pollutants detection, *Appl. Surf. Sci.*, 2023, **613**, 156092, DOI: [10.1016/j.apsusc.2022.156092](https://doi.org/10.1016/j.apsusc.2022.156092).

79 S. Lin, X. Fang, G. Fang, F. Liu, H. Dong, H. Zhao, J. Zhang and B. Dong, Ultrasensitive detection and distinction of pollutants based on SERS assisted by machine learning algorithms, *Sens. Actuators, B*, 2023, **384**, 133651, DOI: [10.1016/j.snb.2023.133651](https://doi.org/10.1016/j.snb.2023.133651).

80 C. Li, B. Man, C. Zhang, J. Yu, G. Liu, M. Tian, Z. Li, X. Zhao, Z. Wang, W. Cui, T. Wang, J. Wang, X. Lin and S. Xu, Strong plasmon resonance coupling in micro-extraction SERS



membrane for *in situ* detection of molecular aqueous solutions, *Sens. Actuators, B*, 2024, **398**, 134767, DOI: [10.1016/j.snb.2023.134767](https://doi.org/10.1016/j.snb.2023.134767).

81 Y. Fan, S. Wang and F. Zhang, Optical Multiplexed Bioassays for Improved Biomedical Diagnostics, *Angew. Chem.*, 2019, **131**, 13342–13353, DOI: [10.1002/ANGE.201901964](https://doi.org/10.1002/ANGE.201901964).

82 X. Tian, L. Zhang, M. Yang, L. Bai, Y. Dai, Z. Yu and Y. Pan, Functional magnetic hybrid nanomaterials for biomedical diagnosis and treatment, *Wiley Interdiscip. Rev.: Nanomed. Nanobiotechnol.*, 2018, **10**, e1476, DOI: [10.1002/WNAN.1476](https://doi.org/10.1002/WNAN.1476).

83 H. Lee, B. Koo, A. Chattopadhyay, R. K. Neerukatti and K. C. Liu, Damage detection technique using ultrasonic guided waves and outlier detection: Application to interface delamination diagnosis of integrated circuit package, *Mech. Syst. Signal. Process.*, 2021, **160**, 107884, DOI: [10.1016/j.ymssp.2021.107884](https://doi.org/10.1016/j.ymssp.2021.107884).

84 H. Kumar, N. Kumari and R. Sharma, Nanocomposites (conducting polymer and nanoparticles) based electrochemical biosensor for the detection of environment pollutant: Its issues and challenges, *Environ. Impact Assess. Rev.*, 2020, **85**, 106438, DOI: [10.1016/J.EIAR.2020.106438](https://doi.org/10.1016/J.EIAR.2020.106438).

85 J. Najeeb, U. Farwa, F. Ishaque, H. Munir, A. Rahdar, M. F. Nazar and M. N. Zafar, Surfactant stabilized gold nanomaterials for environmental sensing applications – A review, *Environ. Res.*, 2022, **208**, 112644, DOI: [10.1016/J.ENVR.2021.112644](https://doi.org/10.1016/J.ENVR.2021.112644).

86 S. Kogularasu, M. Akilarasan, S. M. Chen, T. W. Chen and B. S. Lou, Urea-based morphological engineering of ZnO; for the biosensing enhancement towards dopamine and uric acid in food and biological samples, *Mater. Chem. Phys.*, 2019, **227**, 5–11, DOI: [10.1016/J.MATCHEMPHYS.2019.01.041](https://doi.org/10.1016/J.MATCHEMPHYS.2019.01.041).

87 H. Chen, L. Zhang, Y. Hu, C. Zhou, W. Lan, H. Fu and Y. She, Nanomaterials as optical sensors for application in rapid detection of food contaminants, quality and authenticity, *Sens. Actuators, B*, 2021, **329**, 129135, DOI: [10.1016/J.SNB.2020.129135](https://doi.org/10.1016/J.SNB.2020.129135).

88 R. A. Halvorson and P. J. Vikesland, Surface-enhanced Raman spectroscopy (SERS) for environmental analyses, *Environ. Sci. Technol.*, 2010, **44**, 7749–7755, DOI: [10.1021/es101228z](https://doi.org/10.1021/es101228z).

89 Y. Yang and Z. D. Deng, Stretchable sensors for environmental monitoring, *Appl. Phys. Rev.*, 2019, **6**, 011309, DOI: [10.1063/1.5085013](https://doi.org/10.1063/1.5085013).

90 R. M. Yadav and P. S. Dobal, Structural and electrical characterization of bamboo-shaped C–N nanotubes–poly ethylene oxide (PEO) composite films, *J. Nanopart. Res.*, 2012, **14**, 1155, DOI: [10.1007/s11051-012-1155-3](https://doi.org/10.1007/s11051-012-1155-3).

91 S. Xu, J. Zhan, B. Man, S. Jiang, W. Yue, S. Gao, C. Guo, H. Liu, Z. Li, J. Wang and Y. Zhou, Real-time reliable determination of binding kinetics of DNA hybridization using a multi-channel graphene biosensor, *Nat. Commun.*, 2017, **8**, 14902, DOI: [10.1038/ncomms14902](https://doi.org/10.1038/ncomms14902).

92 G. Liu, Z. Wang, W. Sun, X. Lin, R. Wang, C. Li, L. Zong, Z. Fu, H. Liu and S. Xu, Robust emission in near-infrared II of lanthanide nanoprobes conjugated with Au (LNPs-Au) for temperature sensing and controlled photothermal therapy, *Chem. Eng. J.*, 2023, **452**, 139504, DOI: [10.1016/j.cej.2022.139504](https://doi.org/10.1016/j.cej.2022.139504).

93 S. Xu, C. Zhang, S. Jiang, G. Hu, X. Li, Y. Zou, H. Liu, J. Li, Z. Li, X. Wang, M. Li and J. Wang, Graphene foam field-effect transistor for ultra-sensitive label-free detection of ATP, *Sens. Actuators, B*, 2019, **284**, 125–133, DOI: [10.1016/J.SNB.2018.12.129](https://doi.org/10.1016/J.SNB.2018.12.129).

94 S. Xu, T. Wang, G. Liu, Z. Cao, L. A. Frank, S. Jiang, C. Zhang, Z. Li, V. V. Krasitskaya, Q. Li, Y. Sha, X. Zhang, H. Liu and J. Wang, Analysis of interactions between proteins and small-molecule drugs by a biosensor based on a graphene field-effect transistor, *Sens. Actuators, B*, 2021, **326**, 128991, DOI: [10.1016/J.SNB.2020.128991](https://doi.org/10.1016/J.SNB.2020.128991).

95 M. Tian, M. Qiao, C. Shen, F. Meng, L. A. Frank, V. V. Krasitskaya, T. Wang, X. Zhang, R. Song, Y. Li, J. Liu, S. Xu and J. Wang, Highly-sensitive graphene field effect transistor biosensor using PNA and DNA probes for RNA detection, *Appl. Surf. Sci.*, 2020, **527**, 146839, DOI: [10.1016/J.APSUSC.2020.146839](https://doi.org/10.1016/J.APSUSC.2020.146839).

96 G. Liu, J. Wei, X. Li, M. Tian, Z. Wang, C. Shen, W. Sun, C. Li, X. Li, E. Lv, S. Tian, J. Wang, S. Xu and B. Zhao, Near-Infrared-Responded High Sensitivity Nanoprobe for Steady and Visualized Detection of Albumin in Hepatic Organoids and Mouse Liver, *Adv. Sci.*, 2022, **9**, 2202505, DOI: [10.1002/advs.202202505](https://doi.org/10.1002/advs.202202505).

97 S. Xu, S. Jiang, C. Zhang, W. Yue, Y. Zou, G. Wang, H. Liu, X. Zhang, M. Li, Z. Zhu and J. Wang, Ultrasensitive label-free detection of DNA hybridization by sapphire-based graphene field-effect transistor biosensor, *Appl. Surf. Sci.*, 2018, **427**, 1114–1119, DOI: [10.1016/J.APSUSC.2017.09.113](https://doi.org/10.1016/J.APSUSC.2017.09.113).

